Simulating Secondary Organic Aerosol in a Regional Air Quality Model Using the Statistical Oxidation Model: 1. Assessing the Influence of Constrained Multi-generational Ageing

Shantanu H. Jathar[1,2], Christopher D. Cappa[2], Anthony S. Wexler[2], John H. Seinfeld[3], and Michael J. Kleeman[2]

[1] Mechanical Engineering, Colorado State University, Fort Collins CO

[2] Civil and Environmental Engineering, University of California, Davis CA

[3] Chemical Engineering, California Institute of Technology, Pasadena CA

Corresponding authors: Christopher D. Cappa (cdcappa@ucdavis.edu) and Michael J. Kleeman (mjkleeman@ucdavis.edu).

Abstract

Multi-generational oxidation of volatile organic compound (VOC) oxidation products can significantly alter the mass, chemical composition and properties of secondary organic aerosol (SOA) compared to calculations that consider only the first few generations of oxidation reactions. However, the most commonly used state-of-the-science schemes in 3-D regional or global models that account for multi-generational oxidation (1) consider only functionalization reactions but do not consider fragmentation reactions; (2) have not been constrained to experimental data; and (3) are added on top of existing parameterizations. The incomplete description of multi-generational oxidation in these models has the potential to bias source apportionment and control calculations for SOA. In this work, we used the Statistical Oxidation Model (SOM) of Cappa and Wilson (2012), constrained by experimental laboratory chamber data, to evaluate the regional implications of multi-generational oxidation considering both functionalization and fragmentation reactions. SOM was implemented into the regional UCD/CIT air quality model and applied to air quality episodes in California and the eastern US. The mass, composition and properties of SOA predicted using SOM were compared to SOA predictions generated by a traditional "two-product" model to fully investigate the impact of explicit and self-consistent accounting of multi-generational oxidation.

Results show that SOA mass concentrations predicted by the UCD/CIT-SOM model are very similar to those predicted by a two-product model when both models use parameters that are derived from the same chamber data. Since the two-product model does not explicitly resolve multi-generational oxidation reactions, this finding suggests that the chamber data used to parameterize the models captures the majority of the SOA mass formation from multi-

generational oxidation under the conditions tested. Consequently, the use of low and high NO_x yields perturbs SOA concentrations by a factor of two and are probably a much stronger determinant in 3-D models than multi-generational oxidation. While total predicted SOA mass is similar for the SOM and two-product models, the SOM model predicts increased SOA contributions from anthropogenic (alkane, aromatic) and sesquiterpenes and decreased SOA contributions from isoprene and monoterpene relative to the two-product model calculations. The SOA predicted by SOM has a much lower volatility than that predicted by the traditional model; resulting in better qualitative agreement with volatility measurements of ambient OA. On account of its lower-volatility, the SOA mass produced by SOM does not appear to be as strongly influenced by the inclusion of oligomerization reactions, whereas the two-product model relies heavily on oligomerization to form low volatility SOA products. Finally, an unconstrained contemporary hybrid scheme to model multi-generational oxidation within the framework of a two-product model in which "ageing" reactions are added on top of the existing two-product parameterization is considered. This hybrid scheme formed at least three times more SOA than the SOM during regional simulations as a result of excessive transformation of semi-volatile vapors into lower volatility material that strongly partitions to the particle phase. This finding suggests that these "hybrid" multi-generational schemes should be used with great caution in regional models.

1. Introduction

Organic aerosol (OA) is generally the dominant component of submicrometer-sized atmospheric particulate matter (Jimenez et al., 2009), which plays an important role in the energy budget of the earth (IPCC, 2007) and the health effects of air pollution (Bernstein et al., 2004). Despite its prominence, OA is the least understood component of atmospheric aerosol. Large-scale chemical transport models are the essential tool to simulate concentration distributions, which are needed to form strategies to mitigate, the climate and health impacts of atmospheric aerosols.

OA is a complex mixture of thousands of different compounds that have a wide range of properties (Goldstein and Galbally, 2007). OA can be directly emitted to the atmosphere in particulate form (so-called primary organic aerosol; POA) or it can be formed *in situ* by the oxidation of volatile organic compounds (VOCs) to yield lower volatility products that condense

into the aerosol phase, so-called secondary organic aerosol (SOA). This latter route is generally the predominant one to form OA. Continuous oxidation of VOCs and their oxidation products yields a broad range of products, including those that have intermediate and low volatility. The importance of such "multi-generational oxidation" on SOA production has been widely established in laboratory chamber experiments (Chacon-Madrid et al., 2010;Chacon-Madrid et al., 2013;Yee et al., 2013;Donahue et al., 2012;Chhabra et al., 2011;Henry and Donahue, 2012). Multi-generational oxidation includes the initial formation of oxidized products of lower volatility as well as the loss of SOA mass after initial formation owing to fragmentation reactions. For example, experiments performed with the Potential Aerosol Mass (PAM) reactor, which aims to simulate prolonged VOC oxidation, are always associated with formation followed by destruction of OA mass (Lambe et al., 2012). Simulations that capture this behavior require inclusion of multi-generational oxidation. In addition to altering predicted SOA mass, inclusion of multi-generational oxidation is expected to alter the oxidation state of OA, which has important repercussions for OA properties (e.g., water uptake, toxicity) (Jimenez et al., 2009).

Traditionally, models of SOA formation in chamber experiments have represented SOA formation from VOCs using two to four surrogate products per VOC, the yields for which have been parameterized to reproduce observed levels of SOA (Odum et al., 1996). These models generally assume that the surrogate products are non-reactive (i.e., do not undergo multi-generational oxidation). These models, whether implemented in "two-product" or "volatility basis set" (VBS) forms (Donahue et al., 2006), generally under-predict ambient concentrations of SOA (Carlton et al., 2010). Some models have used simple chemical schemes to mimic the effects of multi-generational oxidation. While these schemes differ in their details, in essence, they assume that the vapors and the products of each surrogate traditional VOC species react with the hydroxyl radical (OH) to form lower volatility products (Robinson et al., 2007;Pye and Seinfeld, 2010;Baek et al., 2011). Such "ageing" schemes to account for multi-generational oxidation of traditional VOC products share similarities with reaction schemes applied to the oxidation of intermediate-volatility organic compounds (IVOCs) and POA vapors (Robinson et al., 2007). Note that oxidation of IVOCs and POA vapors is assumed to proceed only through these ageing-type reactions, whereas oxidation of the semi-volatile products of traditional VOC precursors is an augmentation to the existing two-product or VBS parameterization. Models that

include these ageing schemes predict SOA mass concentrations that close the gap with measured ambient concentrations of OA mass. As a result, over the past five years, both research and regulatory groups have incorporated these schemes into their 3-D models (e.g., Environmental Protection Agency's Community Multiscale Air Quality Model (CMAQ) (Koo et al., 2014), PMCAMx (Murphy and Pandis, 2009;Tsimpidi et al., 2009), WRF-CHEM (Ahmadov et al., 2012;Lane et al., 2008;Tsimpidi et al., 2009)). These first order SOA schemes have three major mechanistic drawbacks. First, they typically do not account for laboratory evidence of fragmentation of oxygenated organic molecules that can lead to decreases in SOA concentrations (Chacon-Madrid and Donahue, 2011;Henry and Donahue, 2012). Second, they assume that the multi-generational oxidation of products of different anthropogenic VOCs (e.g., alkanes versus aromatics) or different biogenic VOCs (e.g., isoprene versus monoterpenes) share the same reaction mechanism. Finally (and most importantly), these schemes remain under-unconstrained in that they have not been rigorously tested against measurements of multi-generational products (or classes of products) under realistic ambient conditions, and they are typically added on top of existing parameterizations. These concerns apply specifically to the multi-generational oxidation schemes that are commonly applied to traditional VOCs, but these are also relevant to the oxidation schemes associated with IVOCs and POA vapors. Chemically explicit models have seldom been used in 3-D modeling (e.g. Johnson et al. (2006), Chen et al. (2006), Ying and Li (2011)) due to their heavy computational burden, although some studies have used reduced complexity forms for 3-D modeling (e.g. Utembe et al. (2011), Lin et al. (2012)) or have implemented them for box modeling studies (e.g. Lee-Taylor et al. (2011)).

In this work, we use the Statistical Oxidation Model (SOM) of Cappa and Wilson (2012) to model the multi-generational oxidation reactions inherent in SOA formation. The SOM provides an efficient framework to track the experimentally-constrained chemical evolution and gas/particle partitioning of SOA using a carbon and oxygen grid. In Jathar et al. (2015), we detailed the coupling of the SOM with the gas-phase chemical mechanism SAPRC-11 (Carter and Heo, 2013) within the UCD/CIT regional air quality model and used the new model to make predictions over the South Coast Air Basin (SoCAB) in California and the eastern United States (US). Here, we use the UCD/CIT-SOM model to investigate the influence of constrained multi-generational oxidation on the mass concentrations and properties of SOA and contrast those

results against predictions from a traditional two-product model and an unconstrained multi-generational oxidation model.

2. Model Description and Simulations

2.1. Air Quality Model

The UCD/CIT air quality model is a regional chemical transport model (CTM) (Kleeman and Cass, 2001) used here to simulate SOA formation for two geographically-distinct domains and time periods: (1) the state of California simulated at a grid resolution of 24 km followed by a nested simulation over the SoCAB at a grid resolution of 8 km from July 20 to August 2, 2005, and (2) the eastern half of the US simulated at a grid resolution of 36 km from August 20th to September 2nd, 2006. Details about the latest version of the UCD/CIT model are provided in Jathar et al. (2015) and summarized in Table S.1. Briefly, anthropogenic emissions for California were based on the California Regional PM10/PM2.5 Air Quality Study (CRPAQS) inventory of 2000 but scaled to match conditions in 2005. FINN (Fire Inventory for National Center for Atmospheric Research) (Wiedinmyer et al., 2011) and MEGAN (Model of Emissions of Gases and Aerosols from Nature) (Guenther et al., 2006) were used to calculate wildfire and biogenic emissions in California. Anthropogenic and wildfire emissions for the eastern US were based on the 2005 National Emissions Inventory (NEI), and biogenic emissions were estimated using BEIS (Biogenic Emissions Inventory System) version 3. Hourly meteorological fields were generated using the Weather Research and Forecasting (WRF) v3.4 model (www.wrf-model.org). National Center for Environmental Protection's NAM (North American Mesoscale) analysis data were used to set the initial and boundary conditions for WRF. Gas- and particle-phase initial and hourly-varying boundary conditions were based on the results from the global model MOZART-4/NCEP (Emmons et al., 2010). Gas-phase chemistry was modeled using SAPRC-11. In all simulations, POA was treated as non-volatile, yet absorptive, as per the treatment in the regulatory Community Multiscale Air Quality (CMAQ) version 4.7 model (Carlton et al., 2010). As such, contributions of semi-volatile and intermediate volatility organic compound emissions (which are commonly assumed to originate from the evaporation of and co-emitted with POA) to the SOA burden were not considered in this study.

2.2. SOA Models

Four types of SOA models are compared in this work: (1) A "Base" two-product model that is equivalent to the SOA model used in CMAQ and representative of SOA models used in most chemical transport (Carlton et al., 2010) and global climate models (Henze et al., 2008); (2) A modified version of the Base model, "BaseM", which uses the two-product framework, but in which the SOA formation parameters were determined using newer chamber data; (3) A "SOM" model (Cappa and Wilson, 2012) in which multi-generational oxidation is accounted for through semi-explicit representation of progressive generations of gas-phase oxidation of the products and precursors of SOA, and that was parameterized based on the same dataset as the BaseM model; (4) A "cascading" oxidation model, wherein ageing of semi-volatile products was accounted for *a posteriori* using ageing rates derived from separate experiments. All of the SOA models utilize fully dynamic gas/particle partitioning for OA species as in Kleeman and Cass (2001) . The following sub-sections describe the four SOA models. To aid the reader, a conceptual schematic comparing various SOA models (e.g. 2-product, SOM, VBS) is provided in Figure. S.1.

2.2.1. Base

The Base model simulated SOA formation as per the pathways and parameters in CMAQ model version 4.7 (Carlton et al., 2010) from the following gas-phase precursors: long alkanes (ALK5), benzene (BENZENE), low-yield aromatics (ARO1), high-yield aromatics (ARO2), isoprene, monoterpenes (TRP1) and sesquiterpenes (SESQ). The species in parentheses are the model species representing those compounds in SAPRC-11 (the gas-phase chemical mechanism used here). The pathways considered include: (1) oxidation of the above-mentioned precursors to form non-reactive semi-volatile products that partition into the particle-phase (Odum et al., 1996) (the so-called two-product model, where model parameters were previously determined from fitting chamber data); (2) acid enhancement of isoprene SOA (Surratt et al., 2007). SOA formation from aromatics is NO_x dependent; low levels of NO_x result in higher SOA formation and vice-versa. The Base model was extended to include particle-phase oligomerization (Kalberer et al., 2004), for which particle-phase semi-volatile components were converted to non-volatile components with $k_{oligomer} = 9.6 \times 10^{-6}$ s^{-1}. In summary, the Base model was run in two configurations, with and without oligomerization reactions: Base and Base-OLIG.

2.2.2. Base Modified

The "modified" version of the Base model, termed "BaseM" was created to facilitate a true evaluation of multi-generational oxidation in a two-product model framework. The BaseM model: (1) used recent chamber data (Jathar et al., 2015) from California Institute of Technology to determine alternate two-product model parameters; and (2) did not include acid-catalyzed enhancement of isoprene SOA and oligomerization reactions. The two-product fit parameters and data sources are listed in Table S.2. Note that the "long alkane" BaseM parameterization has been developed using experimental results for SOA formation from *n*-dodecane (Loza et al., 2014).

2.2.3. Statistical Oxidation Model

The SOM parameterizes multi-generational oxidation using a two-dimensional carbon-oxygen grid to track the evolution of gas- and particle-phase organic products arising from the oxidation of SOA precursors (Cappa and Wilson, 2012;Cappa et al., 2013;Zhang et al., 2014). This evolution through the SOM grid is VOC-specific and defined by six parameters: (P1-P4) yields of the four products that add 1, 2, 3, and 4 oxygen atoms, respectively, without fragmentation; (P5) the probability of fragmentation; and (P6) the decrease in vapor pressure (or volatility) of the species per addition of oxygen atom. Details of the implementation and parameterization of the SOM model in the UCD-CIT are presented in (Jathar et al., 2015). Briefly, six SOM grids with precursor-specific parameter sets were used to represent SOA formation from the same precursor classes in the Base model. Parameter sets were separately determined from high NO_x (low yield) and low NO_x (high yield) chamber data as the SOM in its current configuration cannot yet account for continuous variation in NO_x. The SOM parameters were completely determined from explicit fitting to chamber data where the number of fit data points greatly exceeded the number of fitting parameters (6). Thus, the SOM model will be referred to as "constrained" multi-generational oxidation. The SOM parameters and data sources are listed in Table S.3.

The SOM model parameters used in the present study were determined without accounting for losses of vapors to chamber walls, which can lead to a substantial underestimation of the actual SOA formation potential of a given precursor (Matsunaga and Ziemann,

2010;Zhang et al., 2014). A companion paper evaluates vapor wall-loss effects on the SOM results (Cappa et al., 2015). The SOM parameter fits were derived using dynamic gas-particle partitioning assuming an accommodation coefficient of unity, which tends to minimize the influence of vapor wall loss (McVay et al., 2014), and thus represents a conservative lower bound of SOA formation. The SOM model was additionally extended to consider the influence of oligomerization reactions by allowing irreversible conversion of particle-phase SOM species into a single non-volatile species using the same $k_{oligomer}$ as in the Base model, referred to as SOM-OLIG. Oligomerization reactions were added *a posteriori* to the SOM model, i.e. oligomerization reactions were not included as part of the data fitting and parameter determination and are included in the present study only as a sensitivity case.

2.2.4. Cascading Oxidation Model

Additional simulations were performed using a contemporary multi-generational oxidation scheme, the Cascading Oxidation Model (COM). The COM builds on the two-product Base model but allows for additional reaction of the semi-volatile products using the scheme of Baek et al. (2011). Briefly, the two semi-volatile products from a given precursor react with OH, with the highest volatility product converted into the lowest volatility product and the lowest volatility product converted to a non-volatile product (see SI Section on Cascading Oxidation Model). Like most other schemes that have thus far been used to represent multi-generational oxidation of SOA from traditional VOCs in 3-D models (Lane et al., 2008), COM does not consider fragmentation reactions, is not fit or constrained to experimental data, and adds these ageing reactions on top of an existing parameterization. The COM model will be referred to as "unconstrained" multi-generational oxidation.

Table 1: Simulations performed in this work.

Simulation	**Description**
Base	Equivalent to Carlton et al. (2010) without oligomerization
Base-OLIG	Equivalent to Carlton et al. (2010)
BaseM (low yield)	two-product model using new high NO_x data (low yield)
BaseM (high yield)	two-product model using new low NO_x data (high yield)
SOM (low yield)	New high NO_x data, no vapor wall losses
SOM (high yield)	New low NO_x data, no vapor wall losses
SOM-OLIG (low yield) and SOM-OLIG (high yield)	SOM with inclusion of oligomerization

COM	Base-OLIG model with added ageing reactions

2.3. Simulations

Table 1 lists the simulations performed in this work. We performed two simulations with the Base model (with and without oligomerization), two with the BaseM model (low and high yield), four with the SOM model (low and high yield and with oligomerization accounted for) and one with the COM model. These nine simulations were performed for both domains: SoCAB and the eastern US. Simulations were performed for 19 days with the first 5 days used for spin up. For the SoCAB, each simulated day using the SOM required approximately 4 h of elapsed time (on 40 Intel i5-3570 processor cores) so a 19-day episode was simulated in less than 4 days. For the eastern US, each simulated day required approximately 9 h of elapsed time so a 19-day episode was simulated in about 8 days. The SOM simulations were approximately four times slower than the BaseM simulations on account of the large number of model species.

3. Results

3.1. Base versus BaseM

Although the main focus of the present study is on understanding the role of multi-generational oxidation in SOA models, it is useful to begin by considering differences between the predictions from Base and BaseM (two-product parameters fit to more recent data sets). The 14-day averaged, precursor-resolved SOA concentrations at two sites in the SoCAB (Los Angeles: urban, Riverside: urban outflow) and at two sites in the eastern US (Atlanta: urban, Smoky Mountains: remote) from Base and BaseM are compared in Figure 1. Base model predictions of total semi-volatile SOA concentrations (i.e. SOA exclusive of oligomers) at all four sites are similar to the BaseM (low yield) model predictions that were parameterized using high-NO_x chamber data. This outcome is perhaps not surprising at Los Angeles, Riverside and Atlanta since these urban areas have higher NO_x levels and, correspondingly, the Base simulations effectively used high-NO_x parameters. While there are slight increases in SOA from some precursors and decreases from others, BaseM, in comparison to Base, predicted negligible contributions from alkane SOA. The general agreement between Base and BaseM (low yield) in rural/remote areas like the Smoky Mountains (where more than three-quarters of the SOA comes from terpene oxidation) also resulted from increases in SOA from some precursors and decreases

from others. These precursor-specific differences are a result of slight differences between the two-product yields for these species in Base (Carlton et al., 2010) and BaseM. The comparison between Base and BaseM suggests that while the newer data might not dramatically affect the SOA concentrations in high-NO_x (or urban) areas — at least those that still have marginal biogenic contributions — the newer data could increase SOA concentrations (factor of ~2) in low-NO_x (or rural/remote) areas. One important difference is that the BaseM parameterizations for mono- and sesquiterpenes indicate a NO_x dependence, whereas the Base parameterizations have no NO_x dependence for these compounds. This has implications for the assessment of anthropogenic influences on biogenic SOA and whether biogenic SOA can, to some extent, be controlled (Carlton et al., 2007). Further, the substantial decrease in alkane SOA concentrations in BaseM compared to Base suggests that the Base alkane parameterization might be over-predicting SOA formation from alkanes, at least those that make up ALK5, making it an even smaller fraction of the total SOA mass.

3.2. Effect of Constrained Multi-Generational Oxidation

3.2.1. SOA Concentrations

Predictions from BaseM and SOM, which were parameterized using the same data, were used to investigate the influence of multi-generational oxidation. Domain-wide, 14-day averaged SOA concentrations from BaseM and SOM for the SoCAB and for the eastern US, along with the ratio of the SOA concentrations between SOM and BaseM, are shown in Figure 2. The SOA concentrations presented are averages of the low-yield and high-yield simulations. Consideration of either the low-yield or high-yield simulations individually affects the details, but not the general conclusions about multi-generational oxidation below, even though the SOA mass concentrations from the high-yield simulations are typically 2-4 times larger than from the low-yield simulations (see Figure S.2). In both the SoCAB and the eastern US, the predicted spatial distribution of SOA is generally similar between BaseM and SOM, with only minor differences evident in some locations. For the SoCAB, the SOA concentrations in SOM are somewhat lower everywhere compared to BaseM, by 10-20% in the Los Angeles metropolitan area (marked by a red box) and by about 20-30% in regions dominated by biogenic SOA (e.g., Los Padres National Forest located in the northwest corner of the simulated domain). Similarly, the SOM predictions for SOA concentrations in the eastern US are 0-20% lower than BaseM

predictions over most of the domain. The urban versus biogenic difference was not evident, probably owing to a coarser grid resolution (36 km for the eastern US versus 8 km for the SoCAB). It appears that multi-generational oxidation does not dramatically increase (from additional functionalization reactions) or decrease (from additional fragmentation reactions) the total SOA concentrations formed from the precursor compounds considered in either region.

In Figure 1, at all sites, the SOM SOA concentrations are roughly the same or slightly higher than the BaseM SOA concentrations for the low-yield simulations but consistently lower for the high-yield simulations, by 18-25%. When averaged, the SOM SOA concentrations are slightly lower than the BaseM simulations, largely due to the lower predictions of SOA from mono-terpene and sesquiterpenes in the SOM high yield simulations. The low- versus high-yield distinction suggests that the SOM-predicted SOA is probably similar to BaseM-predicted SOA in urban areas (low yield or high NO_x) but lower in rural/remote areas (high yield or low NO_x).

The seemingly limited influence of multi-generational oxidation on total SOA concentrations runs counter to the findings from previous work that suggests multi-generational oxidation is an important source of SOA (Robinson et al., 2007;Murphy and Pandis, 2009;Baek et al., 2011;Fast et al., 2014;Dzepina et al., 2009). However, these previous efforts accounted for multi-generational VOC oxidation by adding ageing reactions for semi-volatile products on top of an existing parameterization, similar to the COM model, and thus may suffer from "double counting" to some extent (we will return to this point later). These results also indicate that the two-product model parameterization inherently captures some of the influence of multi-generational oxidation, at least over the timescales and conditions relevant for the SoCAB and the eastern US. This can be understood by considering that, although the two-product model assumes non-reactive products, the chamber-observed SOA formation is dependent on production from all reaction generations, even at short oxidation lifetimes (half to a full day of photochemistry); the extent to which multi-generational oxidation influences the two-product fit parameters will depend on the extent to which later generation products are responsible for the actual SOA formation in a given experiment. In summary, it is possible that the chamber-observed SOA formation accounts for the majority of the multi- generational oxidation reactions that contribute to SOA mass and hence, a two-product approach to model SOA formation would already include the mass-enhancement associated with multi-generational oxidation. However,

such a two-product model may not necessarily accurately represent the chemical composition of SOA

The behavior of SOM vs. BaseM predictions is similar in the SoCAB and the eastern US, with minor differences likely related to the size of the domain and the average atmospheric lifetime of the simulated SOA, differences in the evolution of SOA from the various precursors, and the dominance of certain precursors in different domains. These precursor-specific SOA concentrations are visualized in Figure 1 and listed as domain-wide averages in Table S.4. These results indicate that SOM typically produced more SOA from alkanes (although very little overall) but less from terpenes and isoprene in both the SoCAB and the eastern US, compared to BaseM. For aromatics and sesquiterpenes the concentrations are generally similar between the two models, although slightly greater for sesquiterpenes for the eastern US SOM simulations. The use of the SOM model that inherently accounts for multi-generational oxidation leads to more SOA mass for some compounds (due to enhanced functionalization) but less SOA mass for others (due to fragmentation) compared to a static representation of the semi-volatile products. SOA concentrations in chamber photooxidation experiments have been observed to decrease at longer times for some VOCs, notably isoprene (Chhabra et al., 2011) and alpha-pinene (Henry and Donahue, 2012). Such behavior is captured by SOM but not by BaseM, which does not account for fragmentation. Consequently, SOA concentrations in BaseM can never decrease from reactions. The general similarity in the total simulated SOA from BaseM and SOM results in large part from offsetting trends associated with different SOA precursors. This suggests that the use of constrained multi-generational oxidation SOA models, such as SOM, over two-product models may help to provide a clearer picture of the sources of SOA in a given region, even if the different modeling approaches lead to similar total SOA mass concentrations.

The simulated total OA concentrations (POA+SOA) are compared to ambient OA measurements made at the STN (Speciated Trends Network) and IMPROVE (Interagency Monitoring of Protected Visual Environments) air quality monitoring sites in the SoCAB and the eastern US. (IMPROVE sites tend to be remote and with lower OA concentrations compared to STN sites, which tend to be more urban.) Table 2 lists statistical metrics of fractional bias and fractional error that capture model performance for OA for all simulations for both domains at the STN and IMPROVE sites. The simulated SOA fraction of total OA differs greatly between the SoCAB (~10%) and the eastern US (~80%). Consequently, changes in the amount of SOA

simulated will have a larger influence on the total OA in the eastern US, and thus on the comparison with observations. Despite these differences, there is no substantial change in model performance between Base, BaseM and SOM in either domain, with all simulations under-predicting the total OA. In contrast, COM, which leads to substantial increases in the simulated SOA mass concentrations within both domains (see Section 3.3), improved model performance at the STN and IMPROVE sites for the SoCAB and at the STN sites for the eastern US.

Table 2: Fractional bias and fractional error at STN and IMPROVE sites for the SoCAB and the eastern US for the Base, BaseM (average of low- and high-yield), COM and SOM (average of low- and high-yield) simulations. Green, yellow, and orange shading represent 'good', 'average' and 'poor' model performance (Boylan and Russell, 2006).

Simulation	SoCAB				Eastern US			
	STN		IMPROVE		STN		IMPROVE	
	Frac. Bias	Frac. Error	Frac. Bias	Frac. Error	Frac. Bias	Frac. Error	Frac. Bias	Frac. Error
Base	-62	62	-34	43	-78	89	-10	57
BaseM	-61	62	-30	41	-78	87	-8	57
SOM	-62	63	-33	43	-80	89	-12	55
COM	-28	43	27	50	3	61	85	92

3.2.2. SOA Volatility

The effective volatility of the SOA was characterized for the Base, BaseM and SOM simulations. SOA volatility influences the sensitivity of the SOA to dilution and temperature changes. Since Base, BaseM and SOM use model species that have very different volatilities, as characterized by the species saturation concentration, C^*, volatility distributions were developed in which individual species are grouped into logarithmically spaced bins of effective C^*, referred to as volatility basis set-equivalent (VBS_{eq}) distributions (Donahue et al., 2006). In Figure 3(a,c), we show the normalized, episode-averaged VBS_{eq} distributions of SOA at Los Angeles and Atlanta for the Base, BaseM and SOM simulations. Qualitatively, the SOA VBS_{eq} distributions for Base and BaseM are similar, with the bulk of the gas+particle mass being in the $C^* = 1$ to 1000 μg m^{-3} range. In sharp contrast, the SOA volatility distribution for the SOM simulation had a substantial fraction of SOA mass in the $C^* = 0.0001$ to 1 μg m^{-3} range, much lower than the Base/BaseM simulations. At atmospherically-relevant OA concentrations (1-10 μg m^{-3}), the mass in these low C^* bins would be exclusively in the particle-phase.

It is not possible to compare the simulated volatility distributions to ambient observations since direct measurement of volatility distributions has not been demonstrated for such low C^* species. However, the effective volatility of SOA particles has been experimentally assessed by considering the response of particles to heating in a thermodenuder (Cappa and Jimenez, 2010;Huffman et al., 2009). High volatility species generally evaporate at lower temperatures than low volatility species. The theoretical response of the predicted SOA mass, expressed as the mass fraction remaining (MFR), to heating in a thermodenuder over the range 25 to 105 °C was simulated using the model of Cappa (2010). The *C** values varied with temperature according to the Clausius-Clapeyron equation and the enthalpy of vaporization was assumed to be a function of *C** with $\Delta H_{vap} = 131 - 11 \times log_{10} C^*$. (See SI section Thermodenuder Model.) We plot the results in Figure 3(b,d). At both Los Angeles and Atlanta, differences in the predicted SOA volatility are quite evident. In general, the effective SOA volatility was higher in the Base and BaseM simulations than in the SOM simulations. The SOA from the Base and BaseM simulations is almost entirely evaporated when heated to 70 °C, and some evaporation occurs even at 25 °C as a response to vapor stripping in the denuder. In contrast, the SOA from the SOM simulations did not entirely evaporate until 100 °C and exhibits a more gradual decrease with temperature. The SOM-simulated SOA TD evaporation is much more similar to the behavior observed in both laboratory experiments and field assessments of SOA volatility (Cappa and Jimenez, 2010;Huffman et al., 2009;Lee et al., 2010). This suggests that SOM is producing SOA with more physically realistic properties even though the Base/BaseM and SOM simulations produced similar SOA concentrations.

3.2.3. Influence of Oligomerization

The Base-OLIG model includes an oligomerization pathway in which semi-volatile, condensed-phase material is converted to a non-volatile, yet absorptive material on a fixed timescale. This effectively "pumps" semi-volatile vapors to the particle phase and leads to increased SOA concentrations. It has the additional effect of making the SOA less sensitive to dilution and changes in temperature. To examine the influence of oligomerization, Figure 4 shows predictions of the precursor-resolved SOA concentrations from the Base, Base-OLIG, SOM and SOM-OLIG simulations for Los Angeles and Riverside, CA. The total SOA concentrations in Base-OLIG are ~60% higher than Base but the SOA concentrations in SOM-

OLIG were only ~14% higher than SOM. This difference can be understood through the differences between the SOM and Base volatility distributions for semi-volatile species. For the Base model, a large fraction of the oxidation products have $C^* > 1$ μg m^{-3}, and thus a sizable fraction is in the gas-phase. This gas-phase material can be viewed as potential SOA, and as oligomers are formed this material is converted to actual SOA. For SOM, much of the material has $C^* \leq 1$ μg m^{-3}, and thus most of it is already in the particle phase. Consequently, when it is converted to oligomers only a marginal influence on the total SOA concentration results. Overall, it is evident that the influence of oligomerization on simulated SOA concentrations is tightly linked to the semi-volatile product distribution. This may influence the timescales of SOA formation, since in SOM production of lower volatility material is related to the timescales of gas-phase oxidation, whereas in Base, the specified oligomerization rate coefficient, which is largely under-constrained, controls the timescale of low (essentially non-) volatile material.

3.3. Comparing Constrained Multi-generational Oxidation to Unconstrained Schemes

The 14-day averaged SOA concentrations from the COM, Base, and SOM simulations for the SoCAB and the eastern US are compared in Figure 5. Recall that COM allows for conversion of the semi-volatile products in the Base model to lower-volatility products on top of the original 2-product parameterization. The COM simulations predict a factor of 4 to 8 increase in SOA concentrations over the Base and SOM simulations, attributable to the production of low-volatility and non-volatile SOA from the added oxidation reactions. Because COM, like many *ad hoc* ageing schemes (Simon and Bhave, 2011;Robinson et al., 2007;Pye and Seinfeld, 2010;Baek et al., 2011), lacks fragmentation and adds ageing reactions on top of an existing parameterization, and with sufficient oxidation all semi-volatile products will be converted into non-volatile SOA. This means that the ultimate SOA mass yield is equal to the sum of the mass yields of the individual products, independent of their vapor pressures. Given that SOM inherently accounts for multi-generational oxidation as part of the model parameterization, this comparison clearly suggests that the unconstrained schemes used in the COM simulations form too much SOA and that such schemes are not truly representative of multi-generational oxidation in the atmosphere.

Some previous studies have defended the use of a COM-type model because its implementation improved model performance (Lane et al., 2008;Murphy and Pandis, 2009;Shrivastava et al., 2008), as was also observed here (Table 2). However, given that COM-type models remain generally unconstrained and have been inconsistently applied to different VOC precursor types (e.g. ageing of anthropogenics but not biogenics) (Farina et al., 2010;Lane et al., 2008;Murphy and Pandis, 2009), and since recent testing of a COM-type scheme in the laboratory demonstrated that such schemes do, indeed, lead to over-prediction of SOA mass concentration (Zhao et al., 2015), we suggest that this apparently improved agreement is more likely fortuitous than a true indication of improved representation of atmospheric chemistry. It should be noted that the current study specifically assesses the performance of a COM-type model on the SOA production from traditional VOCs only, exclusive of potential contributions of IVOCs and semi-volatile POA vapors to the SOA burden. Previous studies that have examined the influence of multi-generational oxidation of traditional VOCs using COM-type models have typically combined the effects of VOC ageing and IVOC and POA vapor oxidation (e.g. Murphy and Pandis (2009);Jathar et al. (2011)) together and have not investigated the role of each process separately. Consequently, our results, which isolate the influence of using a COM-type oxidation scheme, suggest COM-type models may be inappropriate for use in regional air quality models even though they can lead to improved model/measurement comparison (Table 2). They also imply that models that employed COM-like schemes have potentially underplayed the role of other important OA formation pathways such as aqueous (aerosol, fog, cloud) processing of water-soluble organics (Ervens et al., 2011) and particle-surface reactions (Liggio et al., 2005;Shiraiwa et al., 2013). Future work to integrate semi-volatile POA treatments with constrained multi-generational ageing schemes like SOM is needed.

4. Discussion

When constrained using the same chamber data, the BaseM (traditional two-product model that does not resolve multi-generational oxidation) and SOM models predict roughly the same SOA mass concentrations and spatial distribution for regional air pollution episodes in the SoCAB and the eastern US. This suggests that the chamber data used to constrain the BaseM and SOM parameterizations presumably already includes a majority of the SOA mass that would be

attributable to multi-generational oxidation. The extent to which multi-generational oxidation influences the production of SOA in a given chamber experiment depends on both the volatility and reactivity of the first-generation products and the time-scale of the experiment (Wilson et al., 2012). If SOA formation is dominated by first-generation products, then explicit accounting for multi-generational ageing will not be important. Alternatively, if most SOA is formed from second-generation products with little direct contribution from first-generation products, than a static representation (such as with the 2-product model) might be sufficient even when multi-generational ageing is, in fact, dominant. But if SOA formation is balanced between contributions from first, second and later generation products, then the extent to which a static representation will capture the influence of multi-generational ageing may be highly variable and sensitive to the experimental conditions and number of oxidation lifetimes. Consequently, the appropriateness of extrapolating static model parameterizations to longer (global atmospheric) timescales remains unclear. The results presented here indicate that the 2-product model does capture the influence of multi-generational ageing as part of the parameterization in terms of mass concentration, at least for the regional episodes considered, but it is also apparent that the simulated SOA properties (e.g. volatility) and the explicit contributions of various SOA types are not fully captured by such simple models.

The BaseM and SOM simulations show that the SOA concentrations in the SoCAB and eastern US vary by a factor of two when using parameterizations developed from low vs. high NO_x chamber experiments. Hence, we can argue that for the present simulations NO_x dependence is a much more important factor for SOA production than multi-generational oxidation. While most 3-D models include schemes to simulate the NO_x dependence of SOA formation, these schemes remain *ad hoc* as they are based on limited experimental measurements and also rely on the ability of the model to accurately predict radical concentrations (RO_2, HO_2) or VOC-to-NO_x ratios. In this work, the model predictions from the low- and high-yield simulations bound the NO_x-dependent uncertainty in SOA concentrations and we recommend that future work examine this issue in much more detail.

SOM predicts a modestly different composition of SOA than BaseM despite similar total mass concentrations of SOA. The composition predicted by SOM has a slightly higher contribution from alkanes, aromatics (anthropogenic) and sesquiterpenes and a lower contribution from isoprene and monoterpenes. These modest differences in the predicted

composition of SOA have implications for understanding the sources of ambient aerosol and eventually the regulation of these sources to achieve compliance with National Ambient Air Quality Standards (NAAQS). These more accurate SOA predictions resolved by chemical families should be tested in epidemiological studies to determine if they are associated with adverse health effects. Additionally, SOM predicted a much lower-volatility SOA than BaseM, and SOM predictions are in better qualitative agreement with ambient thermodenuder measurements of OA volatility. Since the SOA has a much lower volatility, there is very little enhancement (10-15%) with the inclusion of oligomerization reactions, implying that while oligomerization might affect composition, it may not be a source of additional SOA formation as the Base model suggests.

In this work, we consider POA as non-volatile and non-reactive and do not consider SOA contributions from IVOCs or semi-volatile POA vapors. Oxidation of IVOCs and semi-volatile POA vapors (i.e. SVOCs) can lead to the production of new SOA mass, but evaporation of POA leads to a decrease in the total OA mass. To some extent, these effects are offsetting (especially for SVOCs, which do not contribute new carbon mass to a model). To the extent that the loss of POA is balanced exactly by the formation of SOA from IVOCs and 'recycling' of semi-volatile POA vapors, the simulations here represent a scenario in which the total OA mass is conserved, although possibly with the wrong spatial distribution (Robinson et al., 2007). Most efforts to incorporate SOA formation from IVOCs and SVOCs have simulated their oxidation using a version of the VBS model in which multi-generational ageing is implicit, but highly underconstrained and structured in such a way that the ultimate (long time) SOA yield is greater than unity because all mass is converted to low-volatility products and oxygen addition is assumed. The SOM framework provides a way to explicitly account for the influence of multi-generational chemistry in SOA formation experiments that include semi-volatile POA vapors and IVOCs (Gordon et al., 2014a;Gordon et al., 2014b;Gordon et al., 2013;Grieshop et al., 2009a;Grieshop et al., 2009b;Hennigan et al., 2011;Miracolo et al., 2011;Miracolo et al., 2012;Platt et al., 2013;Platt et al., 2014;Nordin et al., 2013;Chirico et al., 2010;Heringa et al., 2011;Tkacik et al., 2014), and thus should be useful for constraining the contribution of these compound classes to the ambient OA budget. In addition, the simulations here do not consider the influence of vapor wall losses on SOA formation. Such losses can influence SOA yields in chambers, and consequently the parameterizations that result from fitting of such chamber data.

The influence of vapor wall losses on simulated ambient SOA and OA concentrations within the SOM framework is examined in a companion paper (Cappa et al., 2015). Ultimately, models like the SOM can be applied to chamber experiments to better understand the role and contribution of POA, IVOCs and vapor wall-losses to total OA.

Finally, the comparison between the constrained SOM and the unconstrained COM (commonly used in large-scale models) suggests that COM may be double counting SOA formation. These simple ageing schemes should be refit to chamber data where all parameters can be matched to observed trends in a self-consistent manner.

5. Acknowledgements

This work was supported by the California Air Resources Board (CARB) under contracts 11-755 and 12-312. Although this work was funded by the CARB, the statements and conclusions are those of the authors and not necessarily those of the CARB.

6. References

Ahmadov, R., McKeen, S. A., Robinson, A. L., Bahreini, R., Middlebrook, A. M., de Gouw, J. A., Meagher, J., Hsie, E. Y., Edgerton, E., Shaw, S., and Trainer, M.: A volatility basis set model for summertime secondary organic aerosols over the eastern United States in 2006, Journal Of Geophysical Research-Atmospheres, 117, D06301, 2012.

Baek, J., Hu, Y., Odman, M. T., and Russell, A. G.: Modeling secondary organic aerosol in CMAQ using multigenerational oxidation of semi-volatile organic compounds, Journal of Geophysical Research: Atmospheres, 116, D22204, 2011.

Bernstein, J. A., Alexis, N., Barnes, C., Bernstein, I. L., Bernstein, J. A., Nel, A., Peden, D., Diaz-Sanchez, D., Tarlo, S. M., and Williams, P. B.: Health effects of air pollution, The Journal of Allergy and Clinical Immunology, 114, 1116-1123, 2004.

Boylan, J. W., and Russell, A. G.: PM and light extinction model performance metrics, goals, and criteria for three-dimensional air quality models, Atmospheric Environment, 40, 4946-4959, 2006.

Cappa, C., and Wilson, K.: Multi-generation gas-phase oxidation, equilibrium partitioning, and the formation and evolution of secondary organic aerosol, Atmospheric Chemistry and Physics, 12, 9505-9528, 2012.

Cappa, C. D.: A model of aerosol evaporation kinetics in a thermodenuder, Atmospheric Measurement Techniques, 3, 579-592, 2010.

580 Cappa, C. D., and Jimenez, J. L.: Quantitative estimates of the volatility of ambient organic
581 aerosol, Atmospheric Chemistry & Physics, 10, 5401-5924, doi:10.5194/acp-10-5409-2010,
582 2010.

583 Cappa, C. D., Zhang, X., Loza, C. L., Craven, J. S., Yee, L. D., and Seinfeld, J. H.: Application
584 of the Statistical Oxidation Model (SOM) to Secondary Organic Aerosol formation from
585 photooxidation of C 12 alkanes, Atmospheric Chemistry and Physics, 13, 1591-1606, 2013.

586 Cappa, C. D., Jathar, S. H., Wexler, A. S., Seinfeld, J., and Kleeman, M. J.: Simulating
587 secondary organic aerosol in a regional air quality model using the statistical oxidation model –
588 Part 2: Assessing the influence of vapor wall losses, Atmospheric Chemistry & Physics
589 Discussions, 15, 30081-30126, 2015.

590 Carlton, A. G., Pinder, R. W., Bhave, P. V., and Pouliot, G. A.: To what extent can biogenic
591 SOA be controlled?, Environmental Science & Technology, 44, 3376-3380, 2007.

592 Carlton, A. G., Bhave, P. V., Napelenok, S. L., Edney, E. O., Sarwar, G., Pinder, R. W., Pouliot,
593 G. A., and Houyoux, M.: Model representation of secondary organic aerosol in CMAQv4. 7,
594 Environmental Science & Technology, 44, 8553-8560, 2010.

595 Carter, W. P., and Heo, G.: Development of revised SAPRC aromatics mechanisms,
596 Atmospheric Environment, 77, 404-414, 2013.

597 Chacon-Madrid, H., and Donahue, N.: Fragmentation vs. functionalization: chemical aging and
598 organic aerosol formation, Atmos. Chem. Phys, 11, 10553-10563, doi:10.5194/acp-11-10553-
599 2011 2011.

600 Chacon-Madrid, H. J., Presto, A. A., and Donahue, N. M.: Functionalization vs. fragmentation:
601 n-aldehyde oxidation mechanisms and secondary organic aerosol formation, Phys. Chem. Chem.
602 Phys., 12, 13975–13982, doi: 10.1039/c0cp00200c, 2010.

603 Chacon-Madrid, H. J., Henry, K. M., and Donahue, N. M.: Photo-oxidation of pinonaldehyde at
604 low NO x: from chemistry to organic aerosol formation, Atmospheric Chemistry and Physics,
605 13, 3227-3236, 2013.

606 Chen, J., Mao, H., Talbot, R. W., and Griffin, R. J.: Application of the CACM and MPMPO
607 modules using the CMAQ model for the eastern United States, Journal of Geophysical Research:
608 Atmospheres (1984–2012), 111, 2006.

609 Chhabra, P. S., Ng, N. L., Canagaratna, M. R., Corrigan, A. L., Russell, L. M., Worsnop, D. R.,
610 Flagan, R. C., and Seinfeld, J. H.: Elemental composition and oxidation of chamber organic
611 aerosol, Atmospheric Chemistry and Physics, 11, 8827-8845, 2011.

612 Chirico, R., DeCarlo, P., Heringa, M., Tritscher, T., Richter, R., Prevot, A., Dommen, J.,
613 Weingartner, E., and Wehrle, G.: Impact of aftertreatment devices on primary emissions and
614 secondary organic aerosol formation potential from in-use diesel vehicles: results from smog
615 chamber experiments, Atmospheric Chemistry and Physics, 10, 11545-11563, 2010.

616 Donahue, N., Robinson, A., Stanier, C., and Pandis, S.: Coupled partitioning, dilution, and
617 chemical aging of semivolatile organics, Environ. Sci. Technol, 40, 2635-2643,
618 doi:10.1021/es052297c, 2006.

619 Donahue, N. M., Henry, K. M., Mentel, T. F., Kiendler-Scharr, A., Spindler, C., Bohn, B.,
620 Brauers, T., Dorn, H. P., Fuchs, H., and Tillmann, R.: Aging of biogenic secondary organic
621 aerosol via gas-phase OH radical reactions, Proceedings of the National Academy of Sciences,
622 109, 13503-13508, 2012.

623 Dzepina, K., Volkamer, R., Madronich, S., Tulet, P., Ulbrich, I., Zhang, Q., Cappa, C., Ziemann,
624 P., and Jimenez, J.: Evaluation of recently-proposed secondary organic aerosol models for a case
625 study in Mexico City, Atmospheric Chemistry and Physics, 9, 5681-5709, doi:10.5194/acp-9-
626 5681-2009, 2009.

627 Emmons, L., Walters, S., Hess, P., Lamarque, J.-F., Pfister, G., Fillmore, D., Granier, C.,
628 Guenther, A., Kinnison, D., and Laepple, T.: Description and evaluation of the Model for Ozone
629 and Related chemical Tracers, version 4 (MOZART-4), Geoscientific Model Development, 3,
630 43-67, 2010.

631 Epstein, S. A., Riipinen, I., and Donahue, N. M.: A semiempirical correlation between enthalpy
632 of vaporization and saturation concentration for organic aerosol., Environmental science &
633 technology, 44, 743-748, 2010.

634 Ervens, B., Turpin, B., and Weber, R.: Secondary organic aerosol formation in cloud droplets
635 and aqueous particles (aqSOA): a review of laboratory, field and model studies, Atmospheric
636 Chemistry and Physics, 11, 11069-11102, 2011.

637 Farina, S. C., Adams, P. J., and Pandis, S. N.: Modeling global secondary organic aerosol
638 formation and processing with the volatility basis set: Implications for anthropogenic secondary
639 organic aerosol, Journal of Geophysical Research, 115, D09202, doi:10.1029/2009JD013046,
640 2010.

641 Fast, J. D., Allan, J., Bahreini, R., Craven, J., Emmons, L., Ferrare, R. A., Hayes, P. L., Hodzic,
642 A., Holloway, J., Hostetler, C. A., Jimenez, J. L., Jonsson, S., Liu, Y., Metcalf, C., Middlebrook,
643 A. M., Novak, J., Pekour, M., Perring, A. E., Russell, L., Sedlacek, A., Seinfeld, J., Setyan, A.,
644 Shilling, J., Shrivastava, M., Springston, S., Song, C., Subramanian, R., Taylor, J. W., Vinoj, V.,
645 Yang, Q., Zaveri, R. A., and Zhang, Q.: Modeling regional aerosol and aerosol precursor
646 variability over California and its sensitivity to emissions and long-range transport during the
647 2010 CalNex and CARES campaigns, Atmospheric Chemistry and Physics, 14, 10013-10060,
648 doi:10.5194/acp-14-10013-2014, 2014.

649 Goldstein, A. H., and Galbally, I. E.: Known and unexplored organic constituents in the earth's
650 atmosphere, Environmental Science & Technology, 41, 1514-1521, doi:10.1021/es072476p,
651 2007.

652 Gordon, T. D., Tkacik, D. S., Presto, A. A., Zhang, M., Jathar, S. H., Nguyen, N. T., Massetti, J.,
653 Truong, T., Cicero-Fernandez, P., Maddox, C., Rieger, P., Chattopadhyay, S., Maldonado, H.,
654 Maricq, M. M., and Robinson, A. L.: Primary Gas- and Particle-Phase Emissions and Secondary

655 Organic Aerosol Production from Gasoline and Diesel Off-Road Engines, Environmental
656 Science & Technology, 47, 14137-14146, 2013.

657 Gordon, T. D., Nguyen, N. T., May, A. A., Presto, A. A., Lipsky, E. M., Maldonado, S.,
658 Chattopadhyay, S., Gutierrez, A., Maricq, M., and Robinson, A. L.: Secondary Organic Aerosol
659 Formed from Light Duty Gasoline Vehicle Exhaust Dominates Primary Particulate Matter
660 Emissions, Atmospheric Chemistry & Physics, 14, 4461-4678, doi:10.5194/acpd-13-23173-
661 2013, 2014a.

662 Gordon, T. D., Nguyen, N. T., Presto, A. A., Lipsky, E. M., Maldonado, S., Maricq, M., and
663 Robinson, A. L.: Secondary organic aerosol production from diesel vehicle exhaust: impact of
664 aftertreatment, fuel chemistry and driving cycle, Atmospheric Chemistry & Physics, 14, 4643-
665 4659, doi:10.5194/acp-14-4643-2014, 2014b.

666 Grieshop, A., Donahue, N., and Robinson, A.: Laboratory investigation of photochemical
667 oxidation of organic aerosol from wood fires 2: analysis of aerosol mass spectrometer data,
668 Atmospheric Chemistry and Physics, 9, 2227-2240, 2009a.

669 Grieshop, A. P., Logue, J. M., Donahue, N. M., and Robinson, A. L.: Laboratory investigation of
670 photochemical oxidation of organic aerosol from wood fires 1: measurement and simulation of
671 organic aerosol evolution, Atmospheric Chemistry and Physics, 9, 1263-1277, 10.5194/acp-9-
672 1263-2009, 2009b.

673 Guenther, A., Karl, T., Harley, P., Wiedinmyer, C., Palmer, P., and Geron, C.: Estimates of
674 global terrestrial isoprene emissions using MEGAN (Model of Emissions of Gases and Aerosols
675 from Nature), Atmospheric Chemistry & Physics, 6, 3181-3210, 2006.

676 Hennigan, C. J., Miracolo, M. A., Engelhart, G. J., May, A. A., Presto, A. A., Lee, T., Sullivan,
677 A. P., McMeeking, G. R., Coe, H., Wold, C. E., Hao, W. M., Gilman, J. B., Kuster, W. C.,
678 Gouw, J., Schichtel, B. A., Collett, J. L., Kreidenweis, S. M., and Robinson, A. L.: Chemical and
679 physical transformations of organic aerosol from the photo-oxidation of open biomass burning
680 emissions in an environmental chamber, Atmospheric Chemistry and Physics, 11, 7669-7686,
681 doi:10.5194/acp-11-7669-2011 2011.

682 Henry, K. M., and Donahue, N. M.: Photochemical aging of α-pinene secondary organic aerosol:
683 effects of OH radical sources and photolysis, The Journal of Physical Chemistry A, 116, 5932-
684 5940, 2012.

685 Henze, D., Seinfeld, J., Ng, N., Kroll, J., Fu, T., Jacob, D., and Heald, C.: Global modeling of
686 secondary organic aerosol formation from aromatic hydrocarbons: high- vs. low-yield pathways,
687 Atmospheric Chemistry and Physics, 8, 2405--2420, 2008.

688 Heringa, M., DeCarlo, P., Chirico, R., Tritscher, T., Dommen, J., Weingartner, E., Richter, R.,
689 Wehrle, G., Prevot, A., and Baltensperger, U.: Investigations of primary and secondary
690 particulate matter of different wood combustion appliances with a high-resolution time-of-flight
691 aerosol mass spectrometer, Atmospheric Chemistry and Physics, 11, 5945-5957, 2011.

692 Huffman, J., Docherty, K., Mohr, C., Cubison, M., Ulbrich, I., Ziemann, P., Onasch, T., and
693 Jimenez, J.: Chemically-resolved volatility measurements of organic aerosol fom different
694 sources., Environmental science & technology, 43, 5351–5357, 2009.

695 IPCC: Climate change 2007: The physical science basis, Agenda, 6, 07, 2007.

696 Jathar, S., Farina, S., Robinson, A., and Adams, P.: The influence of semi-volatile and reactive
697 primary emissions on the abundance and properties of global organic aerosol, Atmospheric
698 Chemistry and Physics, 11, 7727-7746, doi:10.5194/acp-11-7727-2011 2011.

699 Jathar, S. H., Cappa, C. D., Wexler, A. S., Seinfeld, J. H., and Kleeman, M. J.: Multi-
700 generational oxidation model to simulate secondary organic aerosol in a 3-D air quality model,
701 Geosci. Model Dev., 8, 2553-2567, 10.5194/gmd-8-2553-2015, 2015.

702 Jathar, S. H., Cappa, C. D., Wexler, A. S., Seinfeld, J. H., and Kleeman, M. J.: Multi-
703 generational Oxidation Model to Simulate Secondary Organic Aerosol in a 3D Air Quality
704 Model, Geophysical Model Development, accepted for publication.

705 Jathar, S. H., Mahmud, A., Barsanti, K. C., Asher, W., Pankow, J. F., and Kleeman, M. J.: Water
706 uptake and its influence on gas/particle partitioning of secondary organic aerosol in the United
707 States, Atmospheric Environment, submitted.

708 Jimenez, J. L., Canagaratna, M. R., Donahue, N. M., Prevot, A. S. H., Zhang, Q., Kroll, J. H.,
709 DeCarlo, P. F., Allan, J. D., Coe, H., Ng, N. L., Aiken, A. C., Docherty, K. S., Ulbrich, I. M.,
710 Grieshop, A. P., Robinson, A. L., Duplissy, J., Smith, J. D., Wilson, K. R., Lanz, V. A., Hueglin,
711 C., Sun, Y. L., Tian, J., Laaksonen, A., Raatikainen, T., Rautiainen, J., Vaattovaara, P., Ehn, M.,
712 Kulmala, M., Tomlinson, J. M., Collins, D. R., Cubison, M. J., E, Dunlea, J., Huffman, J. A.,
713 Onasch, T. B., Alfarra, M. R., Williams, P. I., Bower, K., Kondo, Y., Schneider, J., Drewnick, F.,
714 Borrmann, S., Weimer, S., Demerjian, K., Salcedo, D., Cottrell, L., Griffin, R., Takami, A.,
715 Miyoshi, T., Hatakeyama, S., Shimono, A., Sun, J. Y., Zhang, Y. M., Dzepina, K., Kimmel, J.
716 R., Sueper, D., Jayne, J. T., Herndon, S. C., Trimborn, A. M., Williams, L. R., Wood, E. C.,
717 Middlebrook, A. M., Kolb, C. E., Baltensperger, U., and Worsnop, D. R.: Evolution of Organic
718 Aerosols in the Atmosphere, Science, 326, 1525-1529, 10.1126/science.1180353, 2009.

719 Johnson, D., Utembe, S. R., Jenkin, M. E., Derwent, R. G., Hayman, G. D., Alfarra, M. R., Coe,
720 H., and McFiggans, G.: Simulating regional scale secondary organic aerosol formation during
721 the TORCH 2003 campaign in the southern UK, Atmospheric Chemistry and Physics, 6, 403-
722 418, 2006.

723 Kalberer, M., Paulsen, D., Sax, M., Steinbacher, M., Dommen, J., Prevot, A. S. H., Fisseha, R.,
724 Weingartner, E., Frankevich, V., Zenobi, R., and Baltensperger, U.: Identification of polymers as
725 major components of atmospheric organic aerosols, Science, 303, 1659-1662,
726 10.1126/science.1092185, 2004.

727 Kleeman, M. J., and Cass, G. R.: A 3D Eulerian source-oriented model for an externally mixed
728 aerosol, Environmental Science & Technology, 35, 4834-4848, 2001.

729 Koo, B., Knipping, E., and Yarwood, G.: 1.5-Dimensional volatility basis set approach for
730 modeling organic aerosol in CAMx and CMAQ, Atmospheric Environment, 95, 158-164, 2014.

731 Lambe, A. T., Onasch, T. B., Croasdale, D. R., Wright, J. P., Martin, A. T., Franklin, J. P.,
732 Massoli, P., Kroll, J. H., Canagaratna, M. R., and Brune, W. H.: Transitions from
733 functionalization to fragmentation reactions of laboratory secondary organic aerosol (SOA)
734 generated from the OH oxidation of alkane precursors, Environmental science & technology, 46,
735 5430-5437, 2012.

736 Lane, T. E., Donahue, N. M., and Pandis, S. N.: Simulating secondary organic aerosol formation
737 using the volatility basis-set approach in a chemical transport model, Atmospheric Environment,
738 42, 7439-7451, 2008.

739 Lee-Taylor, J., Madronich, S., Aumont, B., Baker, A., Camredon, M., Hodzic, A., Tyndall, G. S.,
740 Apel, E., and Zaveri, R. A.: Explicit modeling of organic chemistry and secondary organic
741 aerosol partitioning for Mexico City and its outflow plume, Atmospheric Chemistry and Physics,
742 11, 13219-13241, 2011.

743 Lee, B. H., Kostenidou, E., Hildebrandt, L., Riipinen, I., Engelhart, G. J., Mohr, C., DeCarlo, P.
744 F., Mihalopoulos, N., Prevot, A. S. H., and Baltensperger, U.: Measurement of the ambient
745 organic aerosol volatility distribution: application during the Finokalia Aerosol Measurement
746 Experiment (FAME-2008), Atmospheric Chemistry and Physics, 10, 12149-12160, 2010.

747 Liggio, J., Li, S. M., and McLaren, R.: Reactive uptake of glyoxal by particulate matter, Journal
748 of Geophysical Research: Atmospheres (1984–2012), 110, D10304, doi:10.1029/2004JD005113,
749 2005.

750 Lin, G., Penner, J. E., Sillman, S., Taraborrelli, D., and Lelieveld, J.: Global modeling of SOA
751 formation from dicarbonyls, epoxides, organic nitrates and peroxides, Atmospheric Chemistry
752 and Physics, 12, 4743-4774, 2012.

753 Loza, C. L., Craven, J. S., Yee, L. D., Coggon, M. M., Schwantes, R. H., Shiraiwa, M., Zhang,
754 X., Schilling, K. A., Ng, N. L., Canagaratna, M. R., Ziemann, P. J., Flagan, R. C., and Seinfeld,
755 J. H.: Secondary organic aerosol yields of 12-carbon alkanes, Atmospheric Chemistry and
756 Physics, 14, 1423-1439, 2014.

757 Matsunaga, A., and Ziemann, P. J.: Gas-wall partitioning of organic compounds in a Teflon film
758 chamber and potential effects on reaction product and aerosol yield measurements, Aerosol
759 Science and Technology, 44, 881-892, 2010.

760 McVay, R. C., Cappa, C. D., and Seinfeld, J. H.: Vapor–Wall Deposition in Chambers:
761 Theoretical Considerations, Environmental science & technology, 48, 10251-10258, 2014.

762 Miracolo, M., Hennigan, C., Ranjan, M., Nguyen, N., Gordon, T., Lipsky, E., Presto, A.,
763 Donahue, N., and Robinson, A.: Secondary aerosol formation from photochemical aging of
764 aircraft exhaust in a smog chamber, Atmos. Chem. Phys, 11, 4135-4147, doi:10.5194/acp-11-
765 4135-2011, 2011.

766 Miracolo, M. A., Drozd, G. T., Jathar, S., Presto, A. A., Lipsky, E., Corporan, E., and Robinson,
767 A.: Fuel composition and secondary organic aerosol formation: gas-turbine exhaust and
768 alternative aviation fuels, Environmental Science & Technology, 46, 8493-8501,
769 doi:10.1021/es300350c, 2012.

770 Murphy, B., and Pandis, S.: Simulating the formation of semivolatile primary and secondary
771 organic aerosol in a regional chemical transport model., Environmental science & technology,
772 43, 4722-4728, doi:10.1021/es803168a, 2009.

773 Nordin, E. Z., Eriksson, A. C., Roldin, P., Nilsson, P. T., Carlsson, J. E., Kajos, M. K., Hellén,
774 H., Wittbom, C., Rissler, J., Löndahl, J., Swietlicki, E., Svenningson, B., Bohgard, M., Kulmala,
775 M., Hallquest, M., and Pagels, J. H.: Secondary organic aerosol formation from idling gasoline
776 passenger vehicle emissions investigated in a smog chamber, Atmospheric Chemistry and
777 Physics, 13, 6101-6116, 2013.

778 Odum, J. R., Hoffmann, T., Bowman, F., Collins, D., Flagan, R. C., and Seinfeld, J. H.:
779 Gas/particle partitioning and secondary organic aerosol yields, Environmental Science &
780 Technology, 30, 2580-2585, 1996.

781 Platt, S. M., El Haddad, I., Zardini, A. A., Clairotte, M., Astorga, C., Wolf, R., Slowik, J. G.,
782 Temime-Roussel, B., Marchand, N., Ježek, I., Drinovec, L., Močnik, G., Möhler, O., Richter, M.,
783 Barmet, P., Bianchi, F., Baltensperger, U., and Prévôt, A. S. H.: Secondary organic aerosol
784 formation from gasoline vehicle emissions in a new mobile environmental reaction chamber,
785 Atmospheric Chemistry and Physics, 13, 9141-9158, 2013.

786 Platt, S. M., Haddad, I. E., Pieber, S. M., Huang, R. J., Zardini, A. A., Clairotte, M., Suarez-
787 Bertoa, R., Barmet, P., Pfaffenberger, L., Wolf, R., Slowik, J. G., Fuller, S. J., Kalberer, M.,
788 Chirico, R., dommen, J., astorga, C., Zimmermann, R., Marchand, N., Hellebust, S., Temime-
789 Roussel, B., Baltensperger, U., and Prévôt, A. S. H.: Two-stroke scooters are a dominant source
790 of air pollution in many cities, Nature communications, 5, 2014.

791 Pye, H., and Seinfeld, J.: A global perspective on aerosol from low-volatility organic
792 compounds, Atmos. Chem. Phys, 10, 4377-4401, doi:10.5194/acp-10-4377-2010, 2010.

793 Robinson, A. L., Donahue, N. M., Shrivastava, M. K., Weitkamp, E. A., Sage, A. M., Grieshop,
794 A. P., Lane, T. E., Pierce, J. R., and Pandis, S. N.: Rethinking organic aerosols: Semivolatile
795 emissions and photochemical aging, Science, 315, 1259-1262, 2007.

796 Shiraiwa, M., Yee, L. D., Schilling, K. A., Loza, C. L., Craven, J. S., Zuend, A., Ziemann, P. J.,
797 and Seinfeld, J. H.: Size distribution dynamics reveal particle-phase chemistry in organic aerosol
798 formation, Proceedings of the National Academy of Sciences, 110, 11746-11750, 2013.

799 Shrivastava, M. K., Lane, T. E., Donahue, N. M., Pandis, S. N., and Robinson, A. L.: Effects of
800 gas particle partitioning and aging of primary emissions on urban and regional organic aerosol
801 concentrations, Journal of Geophysical Research-Atmospheres, 113, D18301,
802 doi:10.1029/2007JD009735, 2008.

Simon, H., and Bhave, P. V.: Simulating the degree of oxidation in atmospheric organic particles, Environmental science & technology, 46, 331-339, 2011.

Surratt, J. D., Lewandowski, M., Offenberg, J. H., Jaoui, M., Kleindienst, T. E., Edney, E. O., and Seinfeld, J. H.: Effect of acidity on secondary organic aerosol formation from isoprene, Environmental science & technology, 41, 5363-5369, 2007.

Tkacik, D. S., Lambe, A. T., Jathar, S., Li, X., Presto, A. A., Zhao, Y., Blake, D., Meinardi, S., Jayne, J. T., Croteau, P. L., and Robinson, A. L.: Secondary Organic Aerosol Formation from in-Use Motor Vehicle Emissions Using a Potential Aerosol Mass Reactor, Environmental Science & Technology, 48, 11235-11242, 10.1021/es502239v, 2014.

Tsimpidi, A., Karydis, V., Zavala, M., Lei, W., Molina, L., Ulbrich, I., Jimenez, J., and Pandis, S.: Evaluation of the volatility basis-set approach for the simulation of organic aerosol formation in the Mexico City metropolitan area, Atmos. Chem. Phys, 10, 525-546, doi:10.5194/acp-10-525-2010, 2009.

Utembe, S. R., Cooke, M. C., Archibald, A. T., Shallcross, D. E., Derwent, R. G., and Jenkin, M. E.: Simulating secondary organic aerosol in a 3-D Lagrangian chemistry transport model using the reduced Common Representative Intermediates mechanism (CRI v2-R5), Atmospheric Environment, 45, 1604-1614, 2011.

Wiedinmyer, C., Akagi, S., Yokelson, R. J., Emmons, L., Al-Saadi, J., Orlando, J., and Soja, A.: The Fire INventory from NCAR (FINN): A high resolution global model to estimate the emissions from open burning, Geoscientific Model Development, 4, 625, 2011.

Wilson, K. R., Smith, J. D., Kessler, S. H., and Kroll, J. H.: The statistical evolution of multiple generations of oxidation products in the photochemical aging of chemically reduced organic aerosol, Physical Chemistry Chemical Physics, 14, 1468-1479, 2012.

Yee, L. D., Kautzman, K. E., Loza, C. L., Schilling, K. A., Coggon, M. M., Chhabra, P. S., Chan, M. N., Chan, A. W. H., Hersey, S. P., and Crounse, J. D.: Secondary organic aerosol formation from biomass burning intermediates: phenol and methoxyphenols, Atmospheric Chemistry and Physics, 13, 8019-8043, 2013.

Ying, Q., and Li, J.: Implementation and initial application of the near-explicit Master Chemical Mechanism in the 3D Community Multiscale Air Quality (CMAQ) model, Atmospheric Environment, 45, 3244-3256, 2011.

Zhang, X., Cappa, C. D., Jathar, S. H., McVay, R. C., Ensberg, J. J., Kleeman, M. J., and Seinfeld, J. H.: Influence of vapor wall loss in laboratory chambers on yields of secondary organic aerosol, Proceedings of the National Academy of Sciences, 111, 5802-5807, 2014.

Zhao, B., Wang, S., Donahue, N. M., Chuang, W., Hildebrandt Ruiz, L., Ng, N. L., Wang, Y., and Hao, J.: Evaluation of One-Dimensional and Two-Dimensional Volatility Basis Sets in Simulating the Aging of Secondary Organic Aerosol with Smog-Chamber Experiments, Environmental Science & Technology, 49, 2245-2254, 10.1021/es5048914, 2015.

841

Figure Captions

Figure 1: 14-day averaged SOA concentrations at Los Angeles (a), Riverside (b), Atlanta (c) and Smoky Mountains (d) for the Base, BaseM, and SOM simulations resolved by the precursor/ pathway.

Figure 2: (a-b) 14-day averaged SOA concentrations in SoCAB for the BaseM and SOM simulations. (c) Ratio of the 14-day averaged SOA concentration from the SOM simulation to that from the BaseM simulation. The BaseM and SOM results are averages of the low yield and high yield simulations. Red box indicates urban areas surrounding Los Angeles.

Figure 3: Volatility distributions of the 14-day averaged gas+particle SOA mass at Los Angeles (a) and Atlanta (c) for the Base, BaseM and SOM simulations. Thermograms that capture the volatility of the 14- day averaged gas+particle SOA mass at Los Angeles (b) and Atlanta (d) for the Base, BaseM and SOM simulations.

Figure 4: 14-day averaged SOA concentrations at (a) Los Angeles and (b) Riverside for the Base, Base- OLIG, SOM, SOM-OLIG simulations resolved by the precursor/pathway.

Figure 5: 14-day averaged SOA concentrations in SoCAB (a-c) and the eastern US (d-f) for the Base, COM and SOM simulations. The SOM results are averages of the low-yield and high-yield simulations.

Figure S.1: Schematic illustrating the differences between some of the different ways of modeling SOA. From top to bottom: the 2-product model; the COM-type model, i.e. 2-product with ageing; the VBS as applied to VOCs with no ageing; the VBS as applied to VOCs with additional ageing; the VBS as applied to S/IVOCs; and the SOM. The black arrows indicate the production of products directly from the parent VOC and the orange arrows indicate ageing reactions, i.e. reactions involving product species. For the SOM, all species are reactive and both functionalization and fragmentation are possible. In the other models that include ageing, only functionalization reactions are included, i.e. reactions that decrease compound vapor pressures.

Figure S.2:14-day averaged SOA concentrations in SoCAB for the BaseM and SOM simulations for the low-yield and high-yield parameterizations.

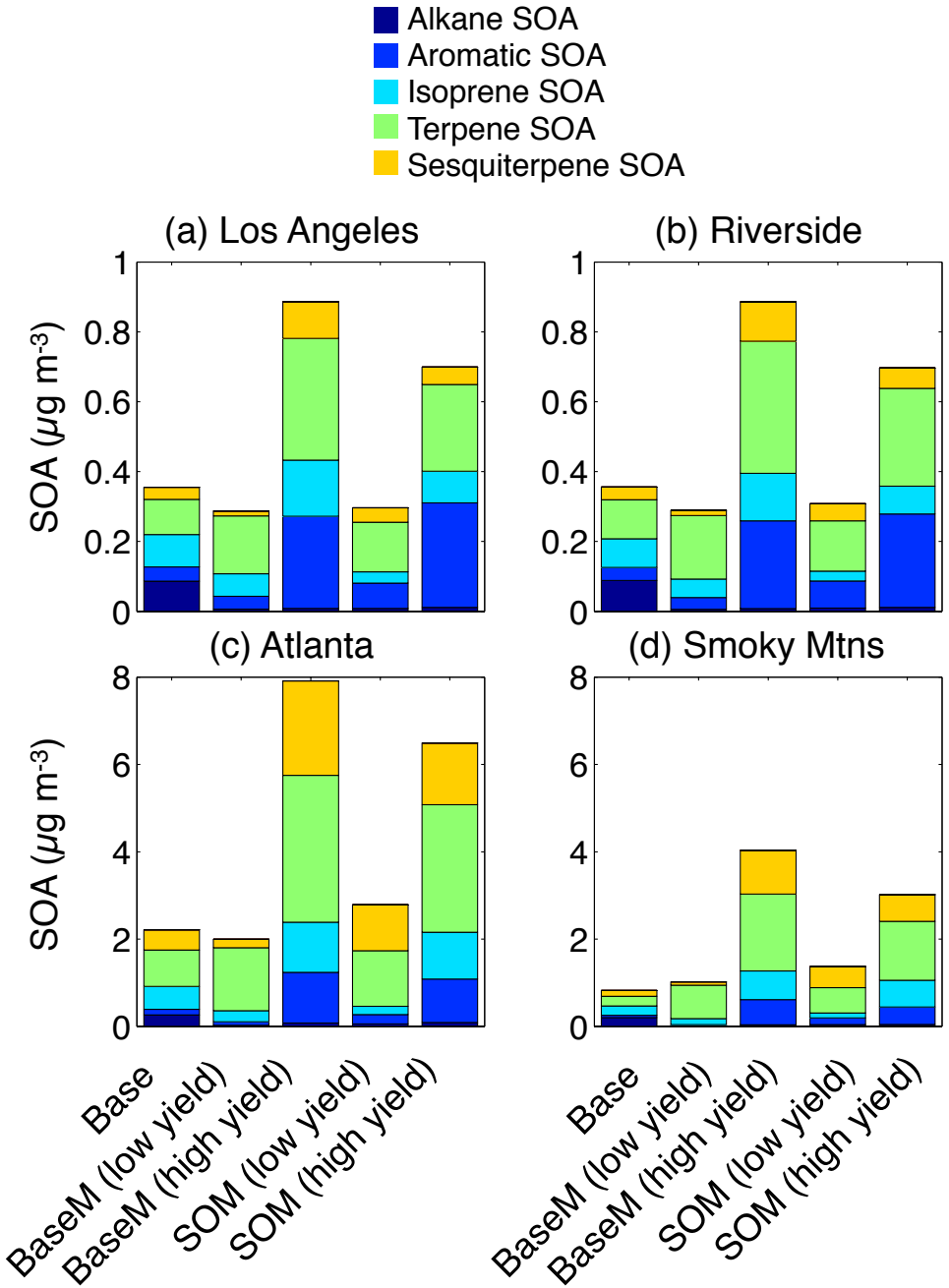
Alkane SOA
Aromatic SOA
Isoprene SOA
Terpene SOA
Sesquiterpene SOA
(a) Los Angeles
(b) Riverside
(c) Atlanta
(d) Smoky Mtns
SOA (μg m-3)
SOA (μg m-3)
0
0.2
0.4
0.6
0.8
1
0
2
4
6
8
Base
BaseM (low yield)
BaseM (high yield)
SOM (low yield)
SOM (high yield)

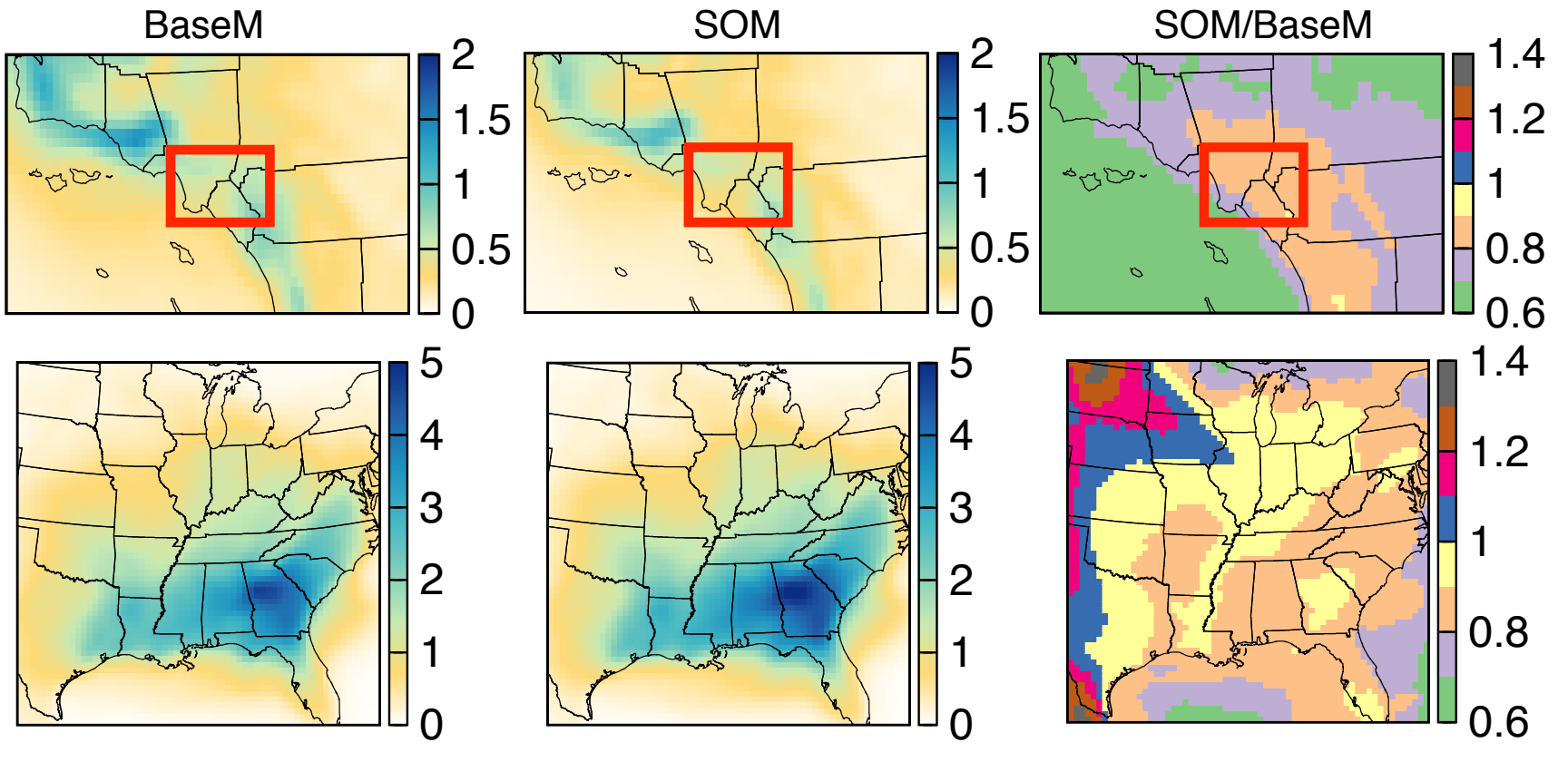
BaseM
SOM
SOM/BaseM
2
1.5
1
0.5
0
2
1.5
1
0.5
0
1.4
1.2
1
0.8
0.6
5
4
3
2
1
0
5
4
3
2
1
0
1.4
1.2
1
0.8
0.6

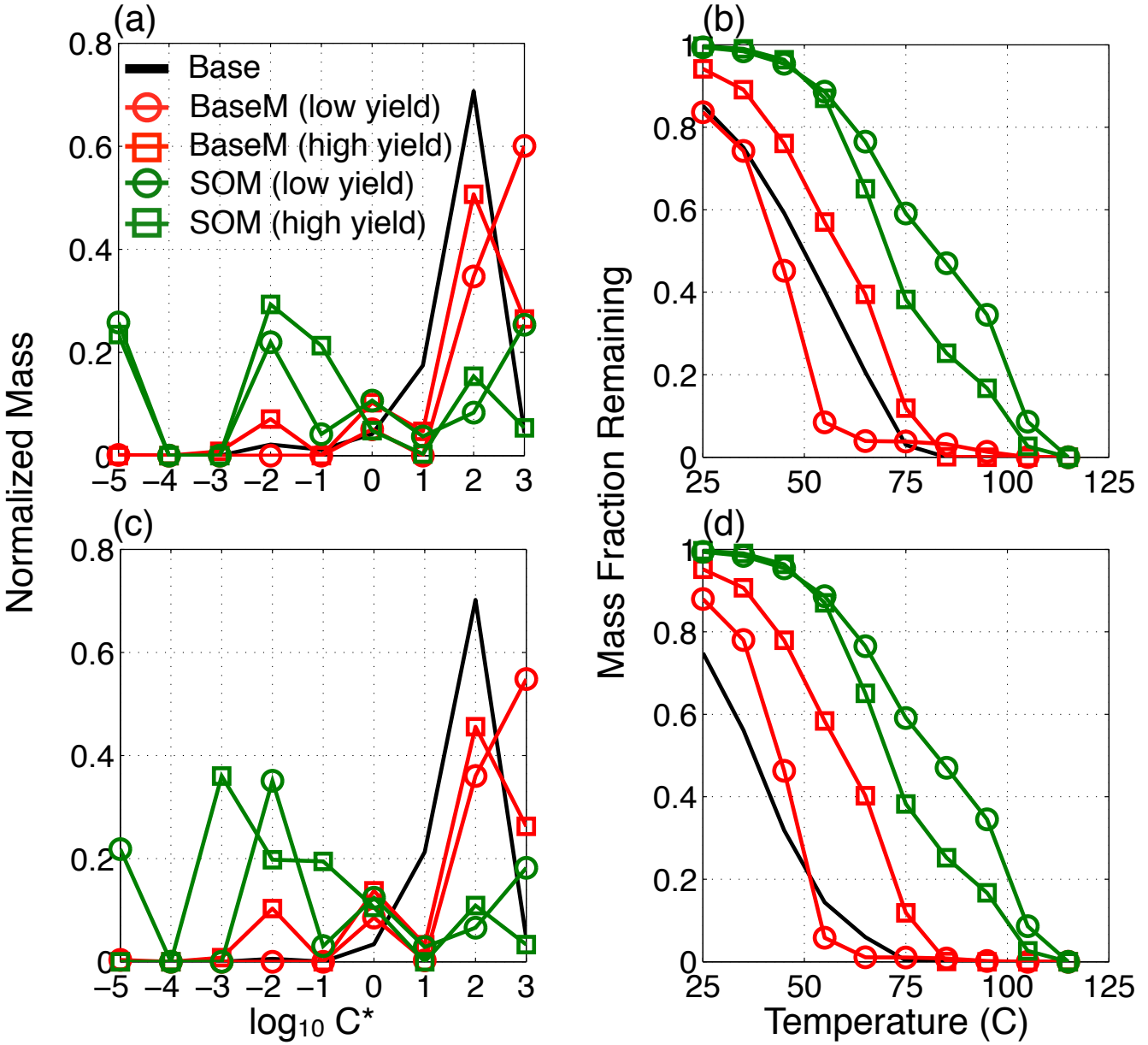
(a)
(b)
(c)
(d)
Base
BaseM (low yield)
BaseM (high yield)
SOM (low yield)
SOM (high yield)
Normalized Mass
Mass Fraction Remaining
log10 C*
Temperature (C)

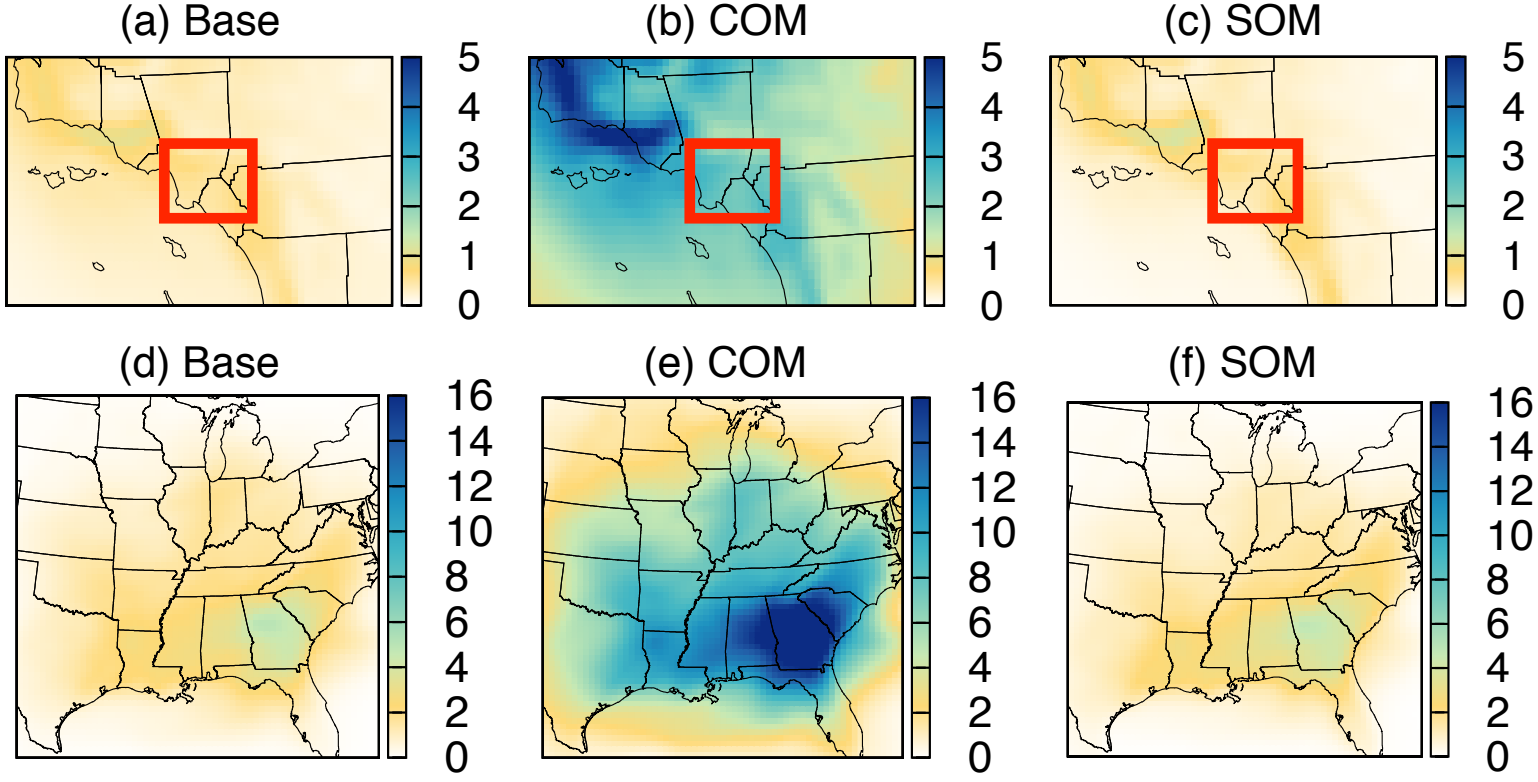
(a) Base
(b) COM
(c) SOM
5
4
3
2
1
0
(d) Base
(e) COM
(f) SOM
16
14
12
10
8
6
4
2
0

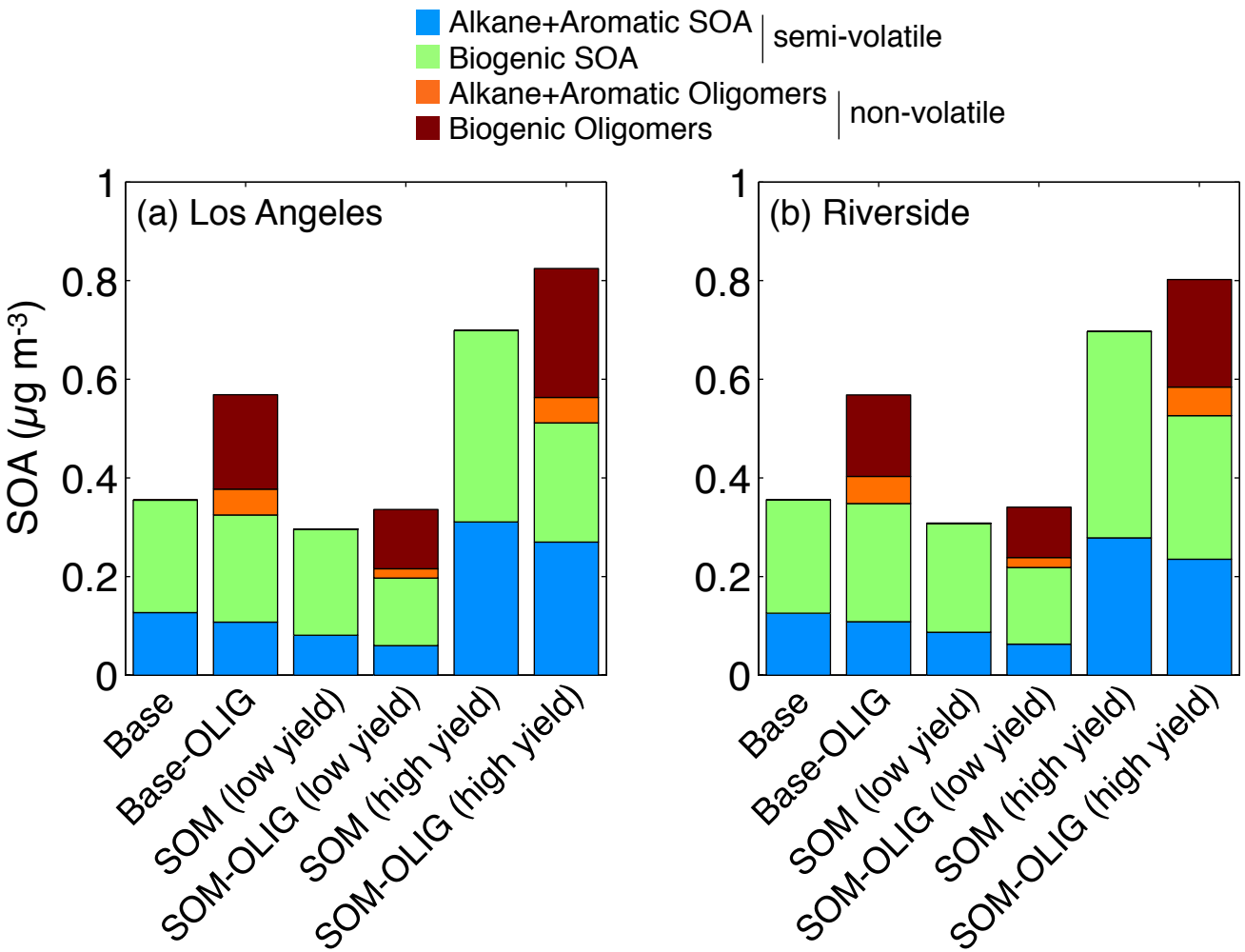
Alkane+Aromatic SOA
Biogenic SOA
Alkane+Aromatic Oligomers
Biogenic Oligomers
semi-volatile
non-volatile
(a) Los Angeles
(b) Riverside
SOA (μg m-3)
0
0.2
0.4
0.6
0.8
1
Base
Base-OLIG
SOM (low yield)
SOM-OLIG (low yield)
SOM (high yield)
SOM-OLIG (high yield)

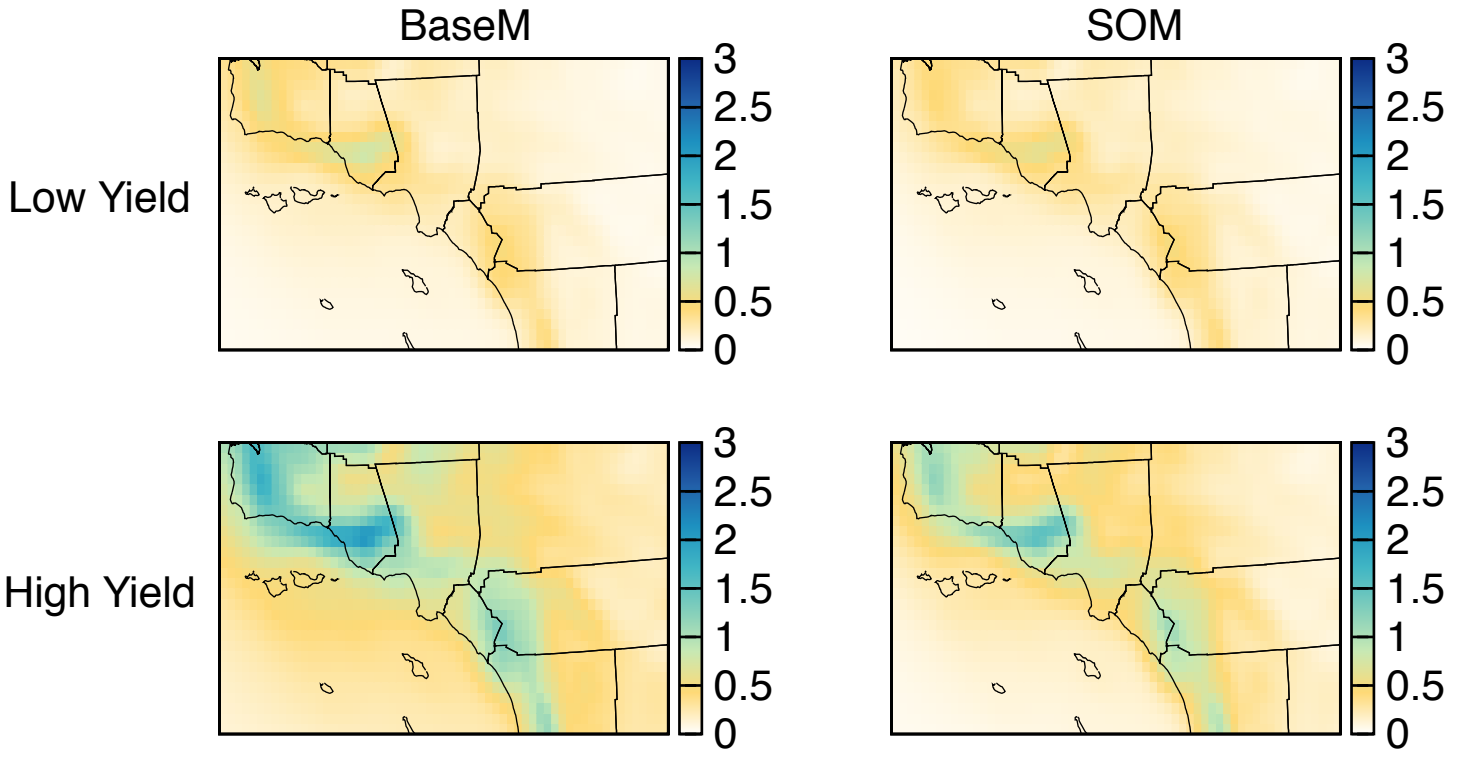
BaseM
SOM
Low Yield
High Yield
3
2.5
2
1.5
1
0.5
0